MCAT Institute
Final Report
93-17

COLORIMETRIC QUALIFICATION OF SHEAR SENSITIVE LIQUID CRYSTAL COATINGS

Joseph J. Muratore, Jr.

August 1993

NCC2-704

MCAT Institute
3933 Blue Gum Drive
San Jose, CA 95127

COLORIMETRIC QUALIFICATION OF SHEAR SENSITIVE LIQUID CRYSTAL COATINGS

Joseph J. Muratore, Jr.

1. BACKGROUND:

The work that has been done to date on the Shear Sensitive Liquid Crystal Project has demonstrated that cholesteric liquid crystal coatings respond to both the direction and magnitude of a shearing force. (1) (See appendix A) The response of the coating is to selectively scatter incident white light into a spectrum of colors. Discernible color changes at a fixed angle of observation and illumination are the result of an applied shear stress. The intention of the study was to be able to convert these observable color patterns from a flow visualization technique into a quantitative tool.

One of the earlier intentions was to be able to use liquid crystals in dynamic flow fields. This was assumed possible because liquid crystals had made it possible to visualize transients in surface shear forces. (1) Although the transients were visualized by color changes to an order one micro second, (2) the time response of a coating to align to a shearing force is dependent on the magnitude of the change between its initial and final states. Unfortunately, the response is not instantaneous. It is for this reason any future attempt at quantifying the magnitude and directions of a shearing force are limited to surface shear stress vector fields in three dimensional steady state flows.

This limitation does not significantly detract from the utility of liquid crystal coatings. The measurement of skin friction in the study of transition on wings, prediction of drag forces, performance assessment and the investigation of boundary layer behavior is of great importance in aerodynamics. There exist numerous examples of techniques for the measurement of surface shear stress. Most techniques require arduous calibrations and necessitate extensive preparation of the receiving surfaces. However, the main draw back of instruments such as Preston tubes, hot films, buried wire gages, and floating element balances is that they only provide a point measurement. (3) The advantages of capturing global shear data would be appreciable when compared with conventional point measurement sensors. It has yet to be determined if a repeatable correlation exists between the measured color of a liquid crystal coating and the magnitude/directional components of a shear vector imposed onto it.

2. SPECTRORADIOMETRIC ANALYSIS:

An initial spectroradiometric analysis of a shear sensitive liquid crystal coating was made in order to quantify observable color changes produced by shear sensitive liquid crystal at different shear stress magnitudes. As figure 2.1 indicates, there is a unique spectral irradiance distribution for any given shear magnitude. Here, an empirically defined relationship between the spectral character of selectively scattered light from a liquid crystal coating and the relative magnitude of an applied shear stress is shown. The data depicted in figure 2.1 was collected from a 15 μm liquid crystal coating covering a flat anodized aluminum plate that was illuminated by a white light source positioned normal to the test surface. A fiber optic probe was used to sample selectively scattered colored light from a point coincident to the center line of a turbulent flow produced by a wall jet (figure 2.2). Light captured by the probe was input to an Oriel Instaspect II spectrophotometer, thereby, measuring the sample's characteristic spectra by plotting irradiance levels as a function of wavelength over the visible spectrum.

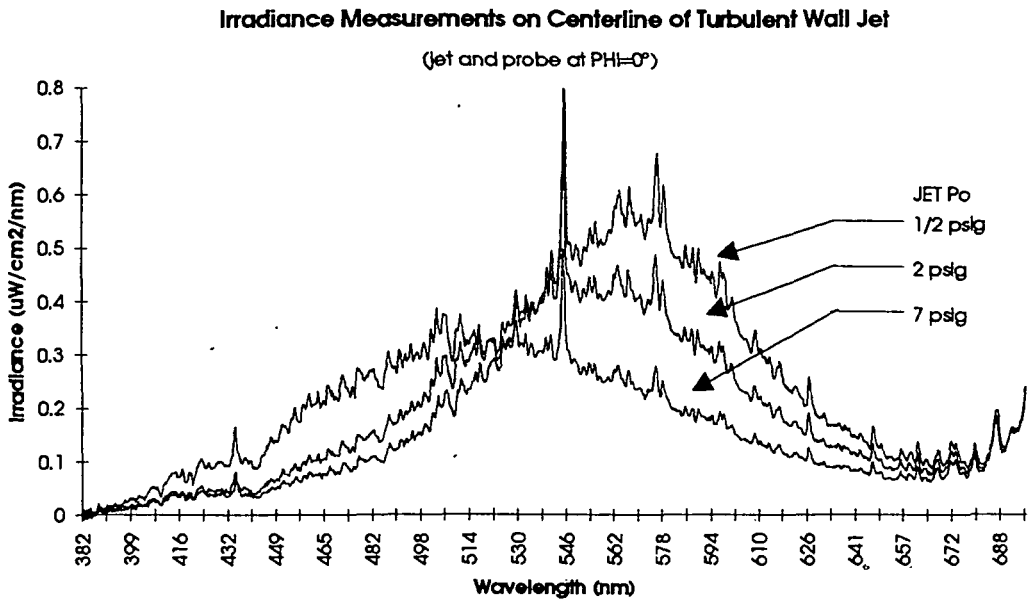

Fig. 2.1 Irradiance Measurements on Centerline of Turbulent Wall Jet with Jet Strength as a Variable.

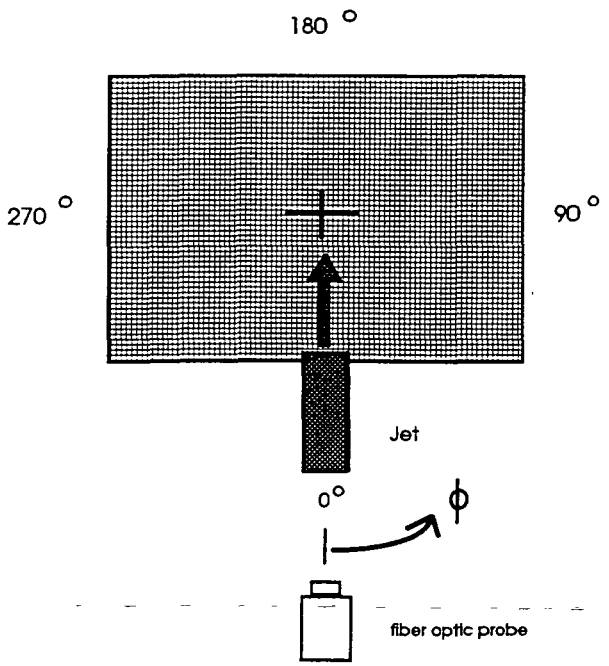

Fig. 2.2 Experimental Setup with Probe at $\phi = 0°$ Elevated to 37° and White Light Source Normal to Test Surface.

3. COLORIMETRIC ANALYSIS:

Although spectral irradiance curves illustrate irradiance changes at each wavelength over the visible spectrum, the amounts of data that would have to be collected in real-time using an imaging spectrometer would be cumbersome even for the lowest image resolutions. (4) It would, therefore, be better to use established colorimetric methods for analysis of the perceivable color changes exhibited by liquid crystal coatings. Colorimetry is the science of color measurement that utilizes trichromatic color matching to quantify a color stimulus. A quantitative measure of color is calculated using the relative amounts of three component primaries that are mix in order to match any spectral color. Thus, any color stimulus can be quantified using three values (tristimulus values).

The human eye, as a detector, collects stimuli from three light sensitive receptor types that line the imaging plane of the eye. The summation of all three stimuli issuing from a single scene element equates to a color's intensity while its chromatic attributes, hue and saturation, are determined by the ratios of the stimuli. The basic principles of color measurement state that a color can be specified with three independent quantities and that color intensity adds linearly. Therefore, a color specification system can be envisioned as involving a three-dimensional color space with any set of convenient coordinates. The coordinates may be transformed mathematically to any other set, if for the sake of measurement or analysis it is deemed appropriate. (5)

The parameters that describe a color are: 1. Spectral reflectivity of the surface being observed, 2. Spectral distribution of the light source illuminating the surface, 3. Spectral sensitivity of the imaging detector. CIE established the following basic quantities for tristimulus colorimetry.

$$X = \int P_\lambda R_\lambda \bar{x}_\lambda \delta\lambda \qquad \text{eq. (1)}$$

$$Y = \int P_\lambda R_\lambda \bar{y}_\lambda \delta\lambda \qquad \text{eq. (2)}$$

$$Z = \int P_\lambda R_\lambda \bar{z}_\lambda \delta\lambda \qquad \text{eq. (3)}$$

X, Y and Z are the definitions for the tristimulus values whose integrations are taken over the range of wavelengths comprising the visible region of the spectrum (400-700 nm). The term P represents the spectral power distribution of illuminant. R is the reflectance or transmittance characteristic of the sample, that is, the portion of the light either reflected from or transmitted through a sample as a function of wavelength. (Note: This quantity is controlled by the liquid crystal coating's response to a shear stress.) The three functions $\bar{x}$, $\bar{y}$, and $\bar{z}$ describe the statistical psycho-physical characteristics of the standard human observer. (6)

3.1 Calculation of the Chromaticity Coordinates:

As a convenience in obtaining two-dimensional maps of color, it is usual to calculate chromaticity coordinates. Using the tristimulus values, one can define chromaticity coordinates. The chromaticity coordinates describe the qualities of a color (i.e., hue and chroma) in addition to its luminance factor. The CIE chromaticity coordinates (x, y and z) are defined as the ratio of

each tristimulus value to the sum X+Y+Z. In effect, x, y, and z represent the relative amounts of three imaginary primaries required to match a particular color. The following equations are used to express each coordinate as a fraction of the sum of the three tristimulus values (X,Y,Z).

$$x = \frac{X}{X+Y+Z} \quad \text{eq. (4)} \qquad y = \frac{Y}{X+Y+Z} \quad \text{eq. (5)} \qquad z = \frac{Z}{X+Y+Z} \quad \text{eq. (6)}$$

Only two of the three coordinates are needed to describe the color since x+y+z=1. [6]

3.2 Plotting Magnitudes of Shear on a Chormaticity Diagram:

Seven samples of the selectively scattered light from the liquid crystal coating were taken using the spectrophotometer each at a relatively higher shear stress magnitude. The chromaticty coordinates were calculated and plotted onto the CIE 1931 (x,y) chromaticity diagram (figure 3.2.1). Each shear stress magnitude plotted at a unique position within the boundaries of the horseshoe-shaped outer boundary of the spectrum locus. This line represents the characteristics of all pure colors in the visible spectrum, as denoted by the corresponding wavelengths labeled on its periphery, and encompasses all perceivable colors. Also plotted on the graph are the coordinates of the white light source (W). This point is used to extrapolate the dominant wavelength (λ_D) on the spectrum locus for each shear magnitude.[5,6] When a line is drawn from the source coordinates and through each data point to the spectrum locus, λ_D is located. As the dominant wavelength correlates to the visual aspect of hue, one has an immediate idea of the appearance of the sampled colors. These experimental results were entirely consistent with the observed color at each shear stress magnitude.

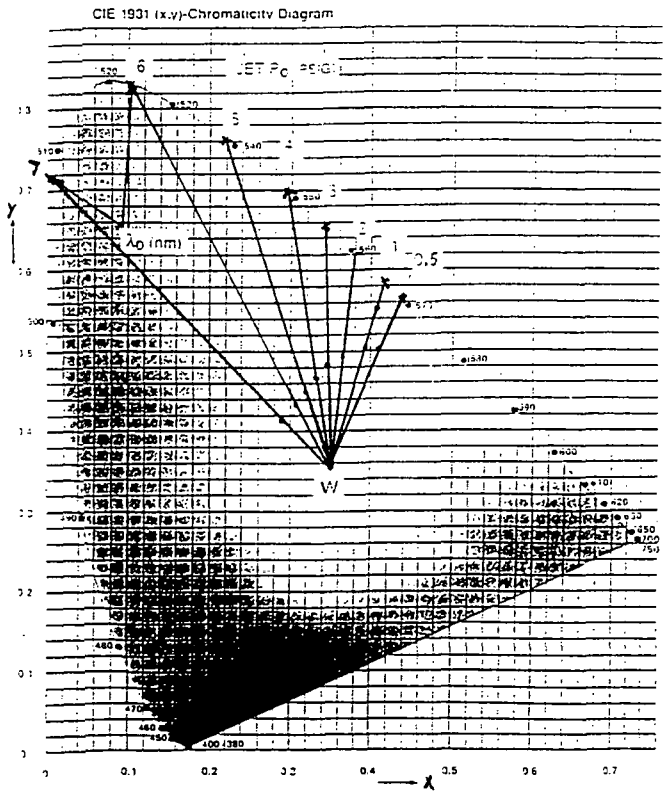

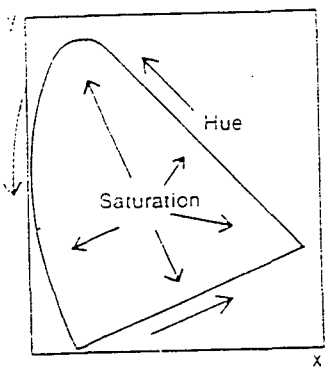

Fig. 3.2.1 Chromaticity Diagram Showing Correlation Between an Extrapolated Dominant Wavelength (hue) and a Relative Shear Stress Magnitude.

4. GLOBAL SHEAR STRESS MEASUREMENTS:

When a liquid crystal coating is subjected to either a varying shear stress or changing flow direction, its color is observed to change. From cursory investigations, a correlation has been found to exist between a magnitude of shear at a fixed point of observation and a measure of a coating's hue subjected to that shearing force.(1) Hue is the attribute of color by means of which a color is perceived to be red, yellow, green, blue, purple, etc. Commercially available color CCD cameras collect light stimulus, as does the human eye, utilizing three sensor sites. It is, therefore, possible to utilize the outputs of a color imaging device to quantify color. The differences in spectral response of each of the camera's imaging sensors compared to those receptors in the human eye can be taken into account during a system calibration procedure. However, such a calibration is superfluous. An instrument whose intent is to correlate a measured color value to shear stress need not perceive color as would the human eye to work just as effectively. One can calculate machine vision tristimulus values by replacing the spectral color matching functions of the human eye in equations 1-3 with those of the color imaging device.

The CIE tristimulus values (X, Y and Z) are defined as the amounts of the three components needed in a three-color additive mixture for matching a color. In calculating these values, the illuminant and the color matching functions of the observer must be denoted. The values obtained are very much dependent on the folowing: 1. The method of integration used, 2. A sample's physical properties and 3. The instrument design used in making the measurements. Tristimulus values are not, therefore, absolute values characteristic of a sample, but relative values dependent on the methodology used to generate them. Approximations can be made of the CIE tristimulus values using a tristimulus colorimeter. However, the filter measurements should then, by convention, be denoted by R, G and B rather than X, Y and Z.

4.1 Imaging System:

The simplified block diagram (figure 4.1.1) illustrates a proposed imaging system that will make real time colorimetric measurements of a scene at each pixel location. The imaging device (#1) requires a unique co-site sampled architecture of the three sensor arrays comprising the imaging head. Co-site sampling is a far superior strategy for accurate color reproduction than the spatial offset architecture found in most broadcast cameras. The precise geometric alignment of the pixel elements using co-site sampling affords equal weighting of the R, G, and B components. The system's A/D converter and real time processor (#3) will translate the component video signals from the imaging head (#1) into RGB tristimulus values at each picture element. Thus, the system will be able to globally record tristimulus values of reflected or transmitted light from a specimen. In effect, the system enables each pixel location to act as a tristimulus colorimeter. An instrument such as this is designed and is properly used for measuring the color difference between like, non-metameric samples.

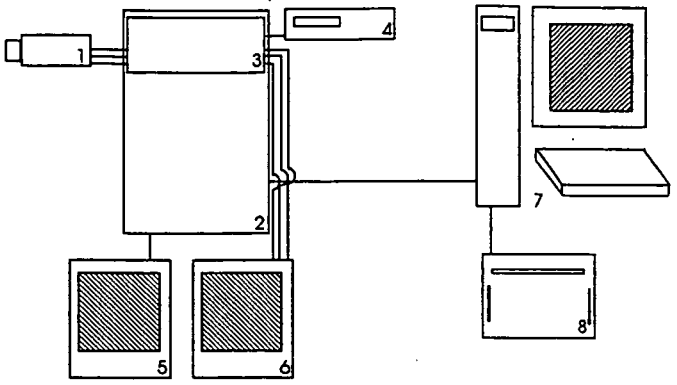

1) 3 Chip CCD Co-site sampled color camera.
2) IBM 486 PC
3) i Matrox IM -1280/a/1/8/F: Base Board
   ii Matrox IMCLD/AT/N: Color Digitizer
   iii Matrox I-RTP/AT : Real Time Processor
4) S-VHS Video Recorder
5) VGA Monitor
6) RGB Mltisync monitor
7) SGI interfaced to color imaging system
8) Hard copy device (i.e. Kodak XL 7700 printer)

Fig. 4.1 .1 RGB Imaging System.

4.2 Calculation of Machine Vision Chromaticity Coordinates:

As a liquid crystal coating is subjected to varying shear stress the perceived color changes. Such changes are describable as a change in hue. There are many color systems that can express a change in hue. These include the RGB, XYZ, CIELAB and CIELUV color systems. (5) Although there are many such systems to choose from, an RGB coordinate system seems best suited for full field colorimetric measurements. In addition, the RGB coordinate system would avoid introducing cumulative errors usually associated with a transformation into another coordinate system. (3) The present scheme for making real time chromaticity measurements utilizes a 24-bit color image processing system. The imaging device utilizes three 756x485 co-site sampled CCD array sensors and outputs three channels of component video (RGB). The separate red, green, and blue analog channels are digitized by an eight bit A/D converter and each pixel in each of the three arrays is assigned value between 0-255. Hence every image pixel can be examined in terms of the RGB components by reduction to its chromaticty coordinates, defined as:

$$r = \frac{R}{R+G+B} \quad \text{eq. (7)} \qquad g = \frac{G}{R+G+B} \quad \text{eq. (8)} \qquad b = \frac{B}{R+G+B} \quad \text{eq. (9)}$$

These coordinates represent points in the chromaticity space of the imaging system. The calibration curves of the shear sensitive liquid crystals would define a specific shear stress at each point of the curve. (3)

This system defined chromaticity space will afford a high level of discrimination for color mapping a shear stress calibration curve. If an equal energy spectrum is input to the imaging system, one can plot the spectrum locus for the system onto the chormaticity diagram. One could then extrapolate the dominant wavelength (a measure of hue) produced by a particular shear stress, in the same manner as described in section 3.1.

4.3 HSI Calculations for Real Time Processing:

Real-time image processing using calculated hue values are possible utilizing an RGB color coordinate system. [5,7] Figure 4.3.1 illustrates the RGB tristimulus space and demonstrates the relation between HSI values and RGB color coordinates. The unit vectors R, G and B define the space, and a color of vector Q corresponds to a point in space with the coordinates (R,G,B). The unit plane in this space is the color triangle containing the chormaticity coordinates (r,g,b) of all perceptible colors. By making the color vector intersect the plane, one can identify chromaticity coordinates of an input stimulus. [8] From the red, green, and blue attributes, a quantification of a color's hue, saturation, and intensity can be calculated geometrically.

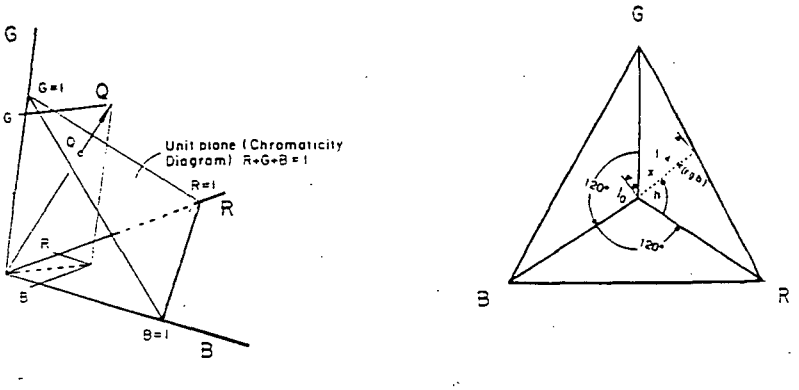

Fig. 4.3.1 (R,G,B)-tristimulus space. A color of Vector Q corresponds to a point in space with the coordinates R,G,B (tristimulus values). The Unit Plane Represents Hue as an Angle Around Its Central axis, and Saturation as the Ratio x/l.

The saturation of a color is depicted by the distance between the center of the triangle to its position within the triangle. The center of the equilateral triangle locates an equal energy stimulus (white point). Therefore, the closer a color plots to the center the more de-saturated the color. The lines connecting the R, G, and B points of the triangle represent the maximum saturation level for any given hue, and the points have a maximum value of 255. The hue is characterized as the angle (θ) which rotates about the white point with the arbitrary placement of R at 0°. The direct hue and intensity conversions from R,G,B attributes are given by:

$$I = R+G+B \qquad \text{eq. (10)}$$

$$H = \begin{cases} \theta & , G \geq B \\ 2\pi - \theta & , G < B \end{cases} \qquad \text{eq. (11)}$$

where:

$$\theta = \cos^{-1} \frac{1/2\,[(R-G)+(R-B)]}{\mathrm{sqr}[(R-G)^2 + (R-B)\,(G-B)]}$$

5 CRITICAL ISSUES / PACING ITEMS:

5.1 Measurement of Hue on a Complex Surface Geometry:

Since relative lighting and view angels affect the color of selectively scattered light, there is a high probability that an aerodynamic test surface with complex geometry will introduce large uncertainties in correlating a hue to a shear stress when using liquid crystal coatings. However, it may be possible to calibrate the system over the entire surface by accounting for the initial static state color at each image pixel. Because of the nonlinear relation between hue to shear stress, it is unlikely that one can quantify a shearing force by calculating the magnitude of a change in hue. Hence, the generation of a unique calibration curve for each effective view angle onto a complex surface geometry is needed to facilitate image data reduction to shear magnitudes. An alternative approach is to investigate the system's tolerance to changes in view angle and restrain the geometry of the test surface to such a limit.

5.2 Intensity Fall Off with an Increase in Shear Magnitude:

Another difficulty associated with shear stress sensitive liquid crystals is the loss of light intensity issuing from the coated surface as an applied shearing force increases. A characteristic that is partially attributable to the removal of crystal coating from the test surface by the flow field. This effect can lead to a decrease in the accuracy of computed r, g, and b values. (9) It is of paramount importance that lighting levels be kept high enough for colors to be accurately assessed. Otherwise, the input color stimulus intensity may be of an insufficient level to provide a high enough signal to noise ratio.

5.3 Software Development:

The Matrox hardware provides a versatile architecture for image processing. There is a complete image library that may be incorporated into any user developed C programming source code. It has been established that NASA through an independent consortium agreement with Stanford University would provide the people with the necessary programming expertise to develop the code for the proposed imaging system. Stanford has already demonstrated a full field colorimetric imaging system used with temperature sensitive-liquid crystal.

5.4 Calibration Rig:

Currently, the experimental set up employs a turbulent wall jet to impose upon a liquid crystal coated test surface a known direction and known relative magnitude of a surface shear stress. A shear stress magnitude can not, however, be directly measured. It is, therefore, imperative that a calibration rig capable of producing known shear stress magnitudes be utilized in the further development of the proposed imaging system. Again, a provision in the existing NASA/Stanford consortium agreement has stipulated a shear stress sensor calibration rig as a deliverable product.

6 EXPANSION OF CURRENT TECHNIQUE:

6.1 Simultaneous Thermographic and Colorimetric Imaging:

Presently, it has been demonstrated using a thermographic camera (band pass of 3.5 to 5 μm) that coatings of shear stress sensitive are transparent to thermal radiation. Hence, isothermal contouring of an aerodynamic test surface through a shear sensitive coating is possible. This makes it theoretically possible for simultaneous full-field measures of shearing forces and thermal conductance to be taken from a test surface. The investigation of the transmission of thermal radiant energy through a liquid crystal coating has been cursory and warrants further investigation. The proposed testing would be to document the spectral transmission of thermal radiation through liquid crystal material over a range of 1 to 5 μm. This will require the use of a specialized spectrophotometer capable of operating over the said range and a rigid substrate material that is largely transparent over this band.

6.2 FALSE COLOR AND VECTOR DIRECTION MAPPING:

The amount of reduced numerical data that will be generated by this proposed full field imaging system is formidable. In theory, over 36,000 data points can be taken in a single image frame. Therefore, the best strategy would be to present the data as an image of the flow field assigning a false color spectrum over the range of shear magnitudes and an arrow for flow direction. (See appendix ii) If thermal information is recorded, the scalar quantity can appear over the region of interest or it can be mapped as a false color image which could be overlaid onto the shear stress flow patterns.

7 CONCLUSIONS:

The intention of the research thus far has been to investigate the feasibility of the development of a full field imaging system to extract global quantitative data from steady state 3D flow fields using shear stress sensitive liquid crystal coatings. The initial results have been encouraging and have suggested that a fully developed technique may include: 1. Recording the directional and magnitude components of a shear vector, 2. Simultaneous thermographic imaging of an aerodynamic test surface to measure the thermal conductance of the test surface and 3. Real-time false color and vector direction mapping of both thermal and shear components of a complex flow field across a test surface. The development of such a full field imaging system operating in real-time is a useful tool in aerodynamics, as it could replace conventional shear stress point sensors with a technique capable of acquiring global shear data.

REFERENCES:

1 Reda, D.C., "Liquid Crystals for Unsteady surface Shear Stress Visualization," AIAA Paper 88-3841, July 1988.

2 Reda, D.C., Muratore Jr., J. J., "Experimental Investigations of the Time and Flow-Direction Responses of Shear-Stress-Sensitive Liquid Crystal Coatings," AIAA Paper 93-0181, 31st Aerospace Sciences Meeting & Exhibit, January 1993.

3 Toy, N., Savory E., and Paskin S., "The Development of a System for Real Time, Full Field Surface Shear Stress Measurements Using Liquid Crystals," 12th Symposium on Turbulence Univ. Missouri, Rolla 1990.

4 Choa, Tien-Hsin, Yu, Jefferey, and Lambert, Jim, "Demonstration of AOTF Imaging Spectrometer," National Aeronautics and Space Administration Technical Support Package, JPL New Technology Report NPO-18410/7942, Jan. 1993

5 Camci C. and Kim K., "A New Hue Capturing Technique for the Quantitative Interpretation of Liquid Crystal Images Used in Convective Heat Transfer Studies," Journal of Turbomachinery, Oct. 1992, vol. 114, pp. 765-775.

6 Billmeyer and Saltzman, Principles of Color Technology 2nd edition, "Describing Color," John Wiley & Sons Inc., New York, 1981, pp. 25-63.

7 Kimura, I., Takamori, T., Ozawa, M., Takenaka, N., and Manabe, Y., "Quantitative Thermal Flow Visualization Using Color Image Processing (Application to a Natural Convection Visualized by Liquid Crystals)," Flow Visualization - 1989, Winter Annual Meeting of The American Society of Mechanical Engineers, Dec 10-15, 1989, pp. 69-76.

8 Wyszecki, G., and Stiles, W. S., Color Science Concepts and Methods, Quantitative Data and Formulae 2nd edition, "Colorimetry", John Wiely & Sons, New York, 1982, pp. 117-153

9 Toy, N., Savory E., and Disimile P.J., "Determination of Surface Temperature and Surface Shear Stress Using Liquid Crystals," ASME Forum on Turbulent Flows Oregon, June 1991.

APPENDIX A

AIAA 93-0181

Experimental Investigations of the Time and Flow-Direction Responses of Shear-Stress-Sensitive Liquid Crystal Coatings

D.C. Reda, J.J. Muratore, Jr. and J.T. Heineck
NASA-Ames Research Center
Moffett Field, CA

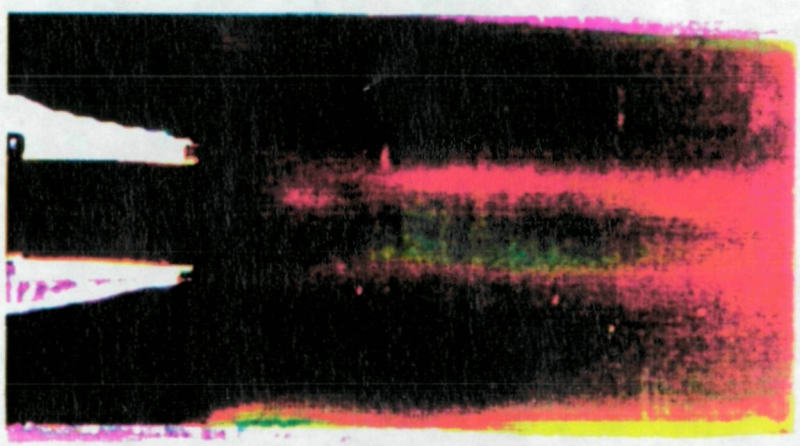

31st Aerospace Sciences Meeting & Exhibit
January 11-14, 1993 / Reno, NV

EXPERIMENTAL INVESTIGATIONS OF THE TIME AND FLOW-DIRECTION RESPONSES OF SHEAR-STRESS-SENSITIVE LIQUID CRYSTAL COATINGS

Daniel C. Reda*, Joseph J. Muratore, Jr.**, and James T. Heineck***

NASA-Ames Research Center
Moffett Field, CA 94035-1000

Abstract

Time and flow-direction responses of shear-stress-sensitive liquid crystal coatings were explored experimentally. For the time-response experiments, coatings were exposed to transient, compressible flows created during the startup and off-design operation of an injector-driven supersonic wind tunnel. Flow transients were visualized with a focusing Schlieren system and recorded with a 1000 frame/sec color video camera. Liquid crystal responses to these changing-shear environments were then recorded with the same video system, documenting color-play response times equal to, or faster than, the time interval between sequential frames (i.e., 1 millisecond). For the flow-direction experiments, a planar test surface was exposed to equal-magnitude and known-direction surface shear stresses generated by both normal and tangential subsonic jet-impingement flows. Under shear, the sense of the angular displacement of the liquid crystal dispersed (reflected) spectrum was found to be a function of the instantaneous direction of the applied shear. This technique thus renders dynamic flow reversals or flow divergences visible over entire test surfaces at image recording rates up to 1 KHz. Extensions of the technique to visualize relatively small changes in surface shear stress direction appear feasible.

Nomenclature

M	Mach number
P_0	Stagnation pressure
Re	Reynolds number per foot
Re_D	Reynolds number based on jet diameter
α_C, α_L	Camera or light angle in plane perpendicular to test surface, measured positive upwards from zero in plane of test surface
$\Delta\alpha$	Change in α
ϕ_C, ϕ_L	Camera or light circumferential angle in plane of test surface, measured positive counter-clockwise from origin shown in Fig. 6
$\Delta\phi$	Change in ϕ

* Senior Research Scientist, Fluid Mechanics Laboratory Branch. Associate Fellow AIAA.
** Research Assistant, MCAT Institute.
*** Scientific and Technical Photographer, Imaging Technology Branch.

Introduction

In fluid mechanics and aerodynamics research, valuable information can be gained from visualization of dynamic surface shear stress patterns on solid bodies immersed in fluid streams. The liquid crystal coating method is a diagnostic technique that can provide areal visualizations of instantaneous shear stress distributions on surfaces in dynamic flowfields with a response that is rapid, continuous and reversible. In the present research, results have been obtained that extend the time response of this technique to order 1 millisecond, and, for the first time, document the shear-stress-direction manifestation capabilities of the technique.

Cholesteric liquid crystals are a highly anisotroptic mesophase that exists between the solid and isotropic-liquid phases of some organic compounds.[1,2] Such materials can exhibit birefringent optical properties characteristic of a crystalline (solid) state. In flow-visualization applications, a mixture of one part liquid crystals to nine parts solvent (presently, Freon) is sprayed onto the aerodynamic surface under study. For small test areas, an artist airbrush is the preferred spray tool. A smooth, flat-black surface is essential for color contrast and must be kept free of grease and other chemical contaminants. Recommended applications (after spray losses) are 10 to 20 ml liquid crystals, measured prior to mixing with the solvent, to each square meter of surface area. The solvent evaporates, leaving a uniform thin film of liquid crystals whose thickness, based on mass conservation and estimated spray losses, is approximately 10 to 20μm (0.0004 to 0.0008 in.).

The molecules within the as-sprayed coating are generally not aligned in a planar texture required to disperse white light into a spectrum, rather, they initially take on a focal-conic texture.[1] Once aligned by shear into the Grandjean plane texture, molecules within the liquid crystal coating selectively scatter incident white light as a spectrum of colors, each color at a discrete angle (orientation) relative to the surface.[1] For "thermochromic" liquid crystal compounds, in the absence of contaminants and electro-magnetic fields, the aligned molecular structure, and thus the light scattering capability of the coating, responds to both temperature and shear stress.[3] For the newly-formulated, shear-stress-sensitive/temperature-

insensitive compounds[4,5],"color play" (i.e., discerned color changes at a fixed angle of observation, for a fixed angle of illumination) results solely from the application of shear stress. The evolution of this technique, for aerodynamic applications, can be ascertained in the writings of Klein[6,7], Holmes[8], Reda[9], Gaudet[10], Bonnett[11], Toy[12], Mee[13], Reda[14], Hall[15], Parmar[16], Toy[17], Reda[18], and Smith.[19]

While it is now known that the technique can be calibrated (under carefully controlled conditions) to measure surface shear stress magnitudes (References 10, 11, 12, 16, and 17) two important issues remain: time response and "directional sensitivities" (to illumination and viewing angles, as well as to the instantaneous shear stress direction).

Parmar[16] investigated the time-response issue by placing a liquid crystal layer (~100μm thick) between two optical glass plates and applying known/transient shear forces via a displacement of one plate. Liquid crystal time constants were measured as a function of the monochromatic wavelength of the incident light. Time constants in the range 10 to 100 milliseconds were generally observed, with minimum values being order 3 milliseconds. The extrapolation (or applicability) of these results to actual fluid mechanic applications, wherein liquid crystal coating thicknesses are an order of magnitude less, remains an open question.

Another approach to characterizing the time-response and/or flow-direction-indication capabilities of the liquid crystal technique is to expose the coating to transient viscous flows of known time scales and/or known shear directions. The oscillating airfoil experiments of Reda[9,14] provided some initial results concerning both issues. New results are presented in subsequent sections.

Time Response

The time response issue was further investigated by exposing coatings of a newly-formulated, shear-stress-sensitive/temperature-insensitive liquid crystal compound[4] (Hallcrest BCN/192) to transient, compressible flows created during the startup and off-design operation of an injector-driven supersonic wind tunnel[20] (see schematic of Figure 1).

In this facility, supersonic injector flows (P_0 = 1 atm, M = 2.4, Re = 3 x 10^6/ft) emanating from above and below the supersonic diffuser exit were used to "pull" the primary flow through the nozzle (P_0 = 0.35 atm, M = 2.5, Re = 10^6/ft); the three merged streams then flowed to a downstream reservoir maintained at 0.55 atm by a vacuum compressor. During these tests, all boundary layers on the sidewall surfaces were turbulent and the settling chamber was completely "open" (i.e., no noise or turbulence suppression devices were installed). Transient flowfield events (unsteady shock wave/boundary layer interactions and supersonic shear layer unsteadiness) responsible for generating transient surface shear stress distributions on the tunnel sidewall (within the field of view delineated in Figure 1) were documented in precursor experiments using a focusing Schlieren system and a high-speed NAC HSV-1000 video camera (to 1000 frames/sec). Observable transients of time scales ≤ 1 millisecond were found to be present.

For the liquid crystal experiments, one sidewall window of the tunnel was removed and replaced with a solid (black) flush-mounted metal insert, which became the test surface. The visible surfaces beneath the three separate streams, and the surface area within the mixing region immediately downstream of the injector/diffuser exit plane, were obliquely illuminated by white light (5600°K with a flicker-free ballast) from the downstream direction (i.e., the principal flow direction was towards the light). The angle of illumination was approximately 45° from the sidewall plane.

Initial attempts at viewing and recording the liquid crystal color-play response were made on a line of sight perpendicular to the test surface. Under these conditions, essentially no color play could be observed. Post-test observations of the shear-aligned liquid crystal coating showed that the spectrum of scattered light (under no-shear conditions) came off the surface in the upstream direction (away from the light) starting with red on the normal, yellow at approximately 30° from normal, green at approximately 45° from normal, followed by "reflected glare", then turquoise (bluish green) "inside" the reflected glare line (see schematic of Figure 2).

For subsequent experiments, the recording devices (movie and/or video cameras) were positioned near the no-shear "mid-spectrum" location, i.e., just before the yellow-to-green transition angle for the shear-aligned coating. Using this camera-alignment procedure, the dynamic surface shear stress patterns on the tunnel sidewall were rendered visible in a most impressive and informative manner. Sample results (individual frames) recorded at 30 frames/second with a standard color video system are shown in Figure 3. The total elapsed time of this tunnel startup sequence was a few seconds. Very high steady-state shear levels beneath the two injector streams caused a loss of color play to occur, i.e., the black surface beneath the coating became visible. Two plausible reasons for this observation exist: either the molecular structure was temporarily forced into an optically-extinct state (homoeotropic texture [1]), or, the dispersed light incident on the camera was shifted outside the visible spectrum. Similar results were seen by Bonnett[11] at high shear rates. Upon removal of shear stress, the entire coating returned to its aligned (Grandjean) texture.

Liquid crystal coating color-play response was also recorded using the NAC Visual Systems HSV-1000 high speed color video system. Liquid crystal coating response time to shear was documented to be equal to, or less than, the time interval between sequential frames recorded at 1 KHz, i.e., 1 millisecond. A color video summarizing these observations is available to interested researchers (request AAV #1373, 9/91). It is also interesting to note that recent research[21,22] into the time response of liquid crystal displays (i.e., the transmission of light through liquid crystal layers exposed to impulsively changed electric fields) has shown achievable liquid crystal response times to be an order of magnitude faster (~0.1 ms).

Results obtained during the present experiments also showed that when the nozzle flow was maintained at a total pressure just below the established "minimum-run" value of ~0.35 atm, random unstarts and restarts of the supersonic diffuser flowfield would occur. In such instances, the shock pattern in and downstream of the diffuser, and the shear layer lateral extent within the mixing region, would all abruptly change. During these highly transient events, the liquid crystal color seen on the diffuser sidewall would also abruptly change from green to red, then red back to green (see frames in Figure 4). Under no-shear conditions (recall Figure 2), these two wavelengths of light (red vs. green) had angular orientations on "opposite sides" of the recording device.

Under steady-state run conditions, reverse flows were known to exist on the supersonic diffuser sidewalls beneath the shock wave/boundary layer interaction region. During momentary unstarts, high-velocity subsonic/attached flows most probably formed, thereby abruptly changing both the shear stress magnitude and direction (by 180^{o}).

Figure 5 shows a two-part schematic that summarizes the apparent flow-direction-indication capabilities of the shear-aligned liquid crystal coating for the special case wherein the light, camera, and principal flow directions are all in the same plane. Further research into this aspect of liquid crystals was then initiated, and results are presented in the following sections.

Shear-Direction Response

Based on the observations discussed above, the following question was posed: Was the sense of the angular displacement of the dispersed (reflected) spectrum relative to a fixed observer dependent on the instantaneous direction of the shear stress "vector" acting on the coating? Two simple "bench-top" experiments were devised to answer this question, one involving a single jet of air impinging normal to a planar test surface, and the other incorporating two tangential jets of equal strength but opposite directions flowing across a planar test surface.

The experimental arrangement was as follows. Clean, dry, pressurized air was fed through two pressure regulators placed in series; output pressure was thus held at 0.5 psig. Air flow was then passed through a single, adjustable valve and tubing to the normal jet, or through a tee and two identical adjustable valves plus tubing (in parallel) to the tangential jets. All jet flows issued from rigid metal tubes with sharp/beveled exits of ID = 0.33" into atmospheric air. Exit velocity was approximately 250 ft./sec. (Re_D ~ 40,000).

For the normal jet experiments, an overhead support frame allowed the jet exit to be held one inch (three jet diameters) above the test surface. Unless otherwise noted, the normal jet stagnation point was at the center of the test surface (a flat-black, 5" by 5" metal plate). For the tangential jet experiments, two separate support frames were positioned on either side of the same test surface, and the beveled jet exits were precisely set to just touch the sharp side edges of the test plate. One tangential jet could be moved laterally along its side of the test plate, allowing the opposite-direction jets to either pass by one another or to impact head on. The "equal strength" of the opposing jets could thus be verified by observing the mean stagnation point location and forcing it (via valve tuning) to be coincident with the plate center.

The test surface was always cleaned and re-sprayed with a new liquid crystal coating (Hallcrest BCN/192) before each experiment. Molecules within the coating were always pre-aligned by shear into the color-play state (the Grandjean texture) through the oblique/multi-directional passage of a pressurized air stream over the test surface.

For the normal jet experiments, the coated test surface rested on a single-column support stand anchored into the top of an optics table. A two-degree-of-freedom, optics-traversing rig (which pivoted about both the vertical and one horizontal axes through the center of the plate) allowed the test surface to be imaged at any ϕ, α combination within the quarter-spherical space encompassing the dispersed spectrum (i.e., on the side of the test surface opposite the light source). For the tangential jet experiments, two fixed/synchronized video cameras were used at symmetric angles to either side of the light plane. In all cases, distances between the cameras and the test surface were kept large compared to the length scales under observation; long-focal-length lenses were used to ensure essentially constant view angles for all points under observation.

White light (5600^{o}K) was supplied from a NAC Visual Systems HMI-1200 unit incorporating a 1200 watt Sylvania PAR64 BriteBeam source with an ultraviolet filter and a flicker-free ballast. The oblique lighting angle was set at $\alpha_L = 25^{o}$ throughout. Three-chip CCD color video cameras produced by SONY and AMPEX were utilized to capture the color images, with signals recorded in BETACAM-SP format.

A color video summarizing the flow-direction-indication experiments is available to interested researchers (request AAV #1433, 9/92). Results of these experiments are presented in the two sections below.

Case 1: Normal Jet Impingement

At any specified radial distance from its stagnation point, a circular jet impinging normal to a flat surface imposes an infinite number of equal-magnitude shear stress vectors on the surface, with angular orientations varying continuously from 0^{o} to 360^{o}. Such a flow field is similar to a "source flow" (see schematic of Figure 6).

Camera sweeps were made through the liquid-crystal-dispersed color space under no-shear conditions prior to recording the shear-induced color patterns for this flowfield. Results are shown in Figures 7 and 8.

For the light source positioned at $\phi_L = 180^{o}$, $\alpha_L = 25^{o}$, a vertical camera sweep in the light plane (α_C from ~10^{o} to ~80^{o} at $\phi_C = 0^{o}$) showed a progression of

colors, from blue at shallow angles, through green and yellow at intermediate angles, to red at the steeper angles (Figure 7). A horizontal camera sweep across the light plane (ϕ_C from -90° to +90° at $\alpha_C = 45°$) showed a different progression of colors, from red on the side, through yellow, to green in the light plane, then inverting in sequence, from green, through yellow, back to red on the other side (Figure 8). Combined results of Figures 7 and 8 document that the no-shear color space is, in fact, three dimensional and symmetric about the light plane.

Shear-induced color patterns beneath the normal-jet-impingement flowfield were then documented using the same horizontal camera sweep employed with Figure 8. Results are shown in Figure 9. A dependency of color play on shear direction was thus clearly documented: some radial shear directions caused a shift from the local no-shear color towards the blue side of the spectrum, while opposing shear directions caused a shift towards the red. The overall "two-lobe" color pattern rotated clockwise as the observer rotated counter-clockwise, yielding mirror images at equal $\Delta\phi$ angles about the light plane. Changing the sense of the camera rotation changed the sense of the color pattern rotation. The perceived "rotation rate" of the two-lobe color pattern with changes in ϕ_C (in either sense), was always greatest as the observer passed through the light plane. For the special case when the camera was in the light plane (middle frame of Figure 9), color shifts for flow away from the observer versus color shifts for flow towards the observer were found to be entirely consistent with the earlier observations of Figures 4 and 5, i.e., the dispersed spectrum appeared to rotate towards the "tail" of the local shear stress vector.

Similar experiments were also conducted using the other five liquid crystal compounds listed in References 4 and 5. All of these shear-stress-sensitive coatings responded in a like manner, i.e., all demonstrated a dependency of color play on shear direction. The normal-jet-impingement flowfield can thus be used to "calibrate" the shear-direction response of any such coating.

Experiments were then undertaken to quantify the three-dimensional color spaces shown in Figures 7, 8, and 9 (for BCN/192). The video camera was removed from the traversing rig and replaced with a 1.6 mm diameter glass fiber optics bundle having a transmission bandwidth of 400 to 1500 nm. This optics probe effectively sampled scattered light only from a point at the center of the test surface (coincident with the center of rotation for the two-degree-of-freedom traversing rig). At every point on a $\Delta\phi = 10°$, $\Delta\alpha = 10°$ grid, the light captured by this probe was input to a spectrophotometer (Oriel Instaspec II diode array system) which dispersed the sampled light into its spectral content, then projected it as a continuous spectrum onto a linear diode-array. The output was a plot of relative light power versus wavelength. The wavelength corresponding to the peak power in each such curve was read and recorded. It should be noted that this single parameter gives an "indication of the color" seen by an observer at each ϕ, α position, but, by itself, does not strictly quantify the color. Given this limitation, numerical values of peak-power wavelength were assigned a color in the data analysis software such that the output color plots were consistent with the video records. Results are shown in Figure 10 as color-coded contours of peak-power wavelength (nanometers) seen by an observer positioned at each point within the quarter-spherical space containing the dispersed spectrum (the $\phi = 0°$ line is at the front/center of each "globe"). A 5° by 5° grid is superimposed on each contour plot and data measured along the $\alpha = 10°$ line were used to plot the unmeasurable values along the $\alpha = 0°$ line. White portions of these plots were not viewable by the probe due to physical constraints.

Under no-shear conditions (the center plot in Figure 10), the reflected color space was found to be three-dimensional and symmetric about the light plane, as described earlier in Figures 7 and 8. Two additional experiments were then conducted to monitor the angular reorientations of this no-shear color space by the imposition of equal-magnitude shear stress vectors having opposite directions. "Shear to the left" (towards $\phi = -90°$) was achieved by offsetting the stagnation point of the normal jet one inch (three jet diameters) to the right of the test plate center; similarly, "shear to the right" (towards $\phi = +90°$) was achieved by a one inch offset of the stagnation point to the left of plate center. The point of observation for the ϕ, α mapping (i.e., the center of rotation for the fiber optic probe) thus remained at the plate center. Equal-magnitude/opposite-direction shear vectors at right angles to the light plane resulted in significant reorientations of the dispersed spectrum (see outside two frames of Figure 10), but these altered color-space patterns were found to be mirror images of one another, consistent with the observations of Figure 9. Similar experiments for shear vectors both towards and away from the light source remain to be done. These initial measurements represent an informative first step in exploring the shear-stress-direction manifestation capabilities of liquid crystal coatings.

Case 2: Tangential Jet Impingement

The other bench-top experiment involved the use of two equal-strength/opposite-direction tangential jets. The first of two lighting/viewing arrangements is shown in Figure 11, where the plane of the jets and the plane of the light source were aligned. The oblique lighting angle remained at $\alpha_L = 25°$ for $\phi_L = 180°$.

The two fixed/synchronized video cameras were positioned at symmetric angles ($\pm$ 55°) to either side of the light plane, and their (matching) elevation angle was set at $\alpha_C = 30°$ so that each camera was in a mid-spectrum position under no-shear conditions (see again the no-shear color space of Figure 10).

The normal-jet-induced color patterns for these two symmetric views about the light plane are redrawn in Figure 12. The observer is at the bottom in both views to be consistent with the simultaneous video frames to be presented below. The reason for re-introducing the normal-jet color patterns is to re-emphasize the fact that such results calibrate the directional response of any liquid crystal coating. One shear vector is shown, corresponding to the transversely-moving jet. According to the shear-direction calibration, shear beneath it should induce blue in both views. Conversely, the

opposite-direction (fixed-jet) shear vector should induce red in both views. Results of the actual experiment are shown in Figures 13 and 14.

Consistent with normal-jet results, the transversely-moving jet (labeled B) induced blue in both views, while the fixed jet (labeled A) induced red in both views (Figure 13). The most vivid colors, however, were seen to occur in the cross-flow directions (perpendicular to the light plane) experienced when the two jets collided head on (Figure 14).

The light plane was thus rotated to be perpendicular to the plane of the jets (Figure 15). As before, two fixed, symmetric, and synchronized views were utilized.

Once again, we redraw the normal-jet-induced color patterns (Figure 16). As before, the observer is at the bottom in both views. Under these lighting and viewing conditions, the moving jet (B) should induce blue in the left view, and, simultaneously, red in the right view. Actual results of the experiment (Figure 17) show that this was indeed the case. Most importantly, opposite flow directions were still seen as different colors to each observer. Comparing Figures 13, 14, and 17, demonstrates that the "strongest color play" (most vivid colors) occurred when the principal flow directions were at right angles to the light plane.

The answer to the question posed earlier was positive. Dynamic surface shear stress directions beneath unsteady/quasi-two-dimensional reversing or diverging (separating or reattaching) flows can now be made visible over an entire test surface at image recording rates up to order 1 KHz. Applications of this technique to unsteady attachment-line flows on the leading edges of wings also appear feasible.

A potential application of this flow-direction-indication technique, to visualize relatively small changes in shear stress direction, is outlined in Figure 18. Again, relying on the normal-jet calibration, proper selection of the lighting and viewing angles could allow the principal flow direction to be aligned with the "split" between the two different-colored lobes. In this case, small changes in surface shear stress direction to one side of the mean-flow vector should induce a yellow-to-blue shift, while, conversely, a small change to the other side of the principal shear vector should induce a yellow-to-red shift. These experiments will be attempted in the near future.

Based on the positive results of the present experiments, a patent on the liquid-crystal, flow-direction-indication technique is being pursued on behalf of the U.S. Government.

Summary

1. For shear-stress-sensitive liquid crystal coatings prealigned by shear into the color-play state (Grandjean plane texture) and obliquely illuminated by white light, the dispersed (reflected) spectrum was found to be a three-dimensional color space symmetric about the light plane.

2. Under shear, the sense of the angular displacement of the dispersed spectrum relative to a fixed observer was found to be a function of the instantaneous direction of the applied surface shear stress.

3. Since normal-jet impingement simultaneously imposes equal-magnitude shear stress vectors encompassing all possible orientations, it provides a simple method to calibrate the shear-direction response of any liquid crystal coating.

4. In general, to best utilize these characteristics of liquid crystal coatings for flow-direction indication, the principal flow direction(s) should be approximately perpendicular to the light plane, the plane of the observer should be offset (rotated) from the light plane, and the view angle within the observation plane should be at a no-shear/mid-spectrum orientation. The technique can also be applied to the special case wherein the light, camera, and principal flow direction(s) are all in the same plane (e.g., operation through a single window) with no loss in signal quality.

5. Using this technique, dynamic flow reversals or flow divergences can now be made visible over an entire test surface at image recording rates up to order 1 KHz.

6. Extensions of the technique to visualize relatively small changes in surface shear stress direction appear feasible.

Acknowledgments

Credit is given to Wade Sisler, Jay Scheibe, Brent Adams, and Tom Reddy of the Imaging Technology Branch, NASA-Ames Research Center, for their important contributions in video recording, frame capturing, and video editing. Credit is given to Doug Edwards of Calspan Corporation for his efforts in designing and fabricating the camera-traversing rig. Credit is given to Tim Archer of Breene Kerr Productions, Mountain View, CA, for his creation of the video graphics used herein. And finally, credit is given to Dr. Mehran Tadjfar, National Research Council Postdoctoral Fellow at NASA-Ames Research Center for his assistance in the applications of the FAST computer software to current data-analyses and color-imaging needs.

References

1. Gray, G. W., "Molecular Structure and the Properties of Liquid Crystals," Academic Press, NY, 1962.

2. Fergason, J. L., "Liquid Crystals," Scientific American, Vol. 211, Aug. 1964, pp. 76-85.

3. Kasagi, N., Moffat, R. J., and Hirata, M., "Liquid Crystals," Chapter 8, Handbook of Flow Visualization, edited by W. J. Yang, Hemisphere Publishing Corp., NY, 1989, pp. 105-124.

4. Parsley, M., "Personal Communication r.e. Hallcrest Liquid Crystal Mixtures BCN/192, BCN/195, BN/R50C and CN/R3," Hallcrest, Liquid Crystal Division, Glenview, IL, Aug. 1991.

5. Terzian, A., "Personal Communication r.e. BDH Liquid Crystal Mixtures TI 511 and TI 622", EM Industries, Advanced Chemicals Division, Hawthorne, NY, Sept. 1989.

6. Klein, E .J., "Liquid Crystals in Aerodynamic Testing," Astronautics and Aeronautics, Vol. 6, July 1968, pp. 70-73.

7. Klein, E. J., and Margozzi, A. P., "Exploratory Investigation on the Measurement of Skin Friction by Means of Liquid Crystals," NASA-TM-X-1774, May 1969.

8. Holmes, B.J., Gall, P.D., Croom, C. C., Manuel, G. S., and Kelliher, W. C., "A New Method for Laminar Boundary Layer Transition Visualization in Flight: Color Changes in Liquid Crystal Coatings," NASA-TM-87666, Jan. 1986.

9. Reda, D. C., "Liquid Crystals for Unsteady Surface Shear Stress Visualization," AIAA Paper 88-3841, July 1988.

10. Gaudet, L., and Gell, T. G., "Use of Liquid Crystals for Qualitative and Quantitative 2-D Studies of Transition and Skin Friction," Royal Aerospace Establishment, TM AERO-2159, London, June 1989.

11. Bonnett, P., Jones, T. V., and McDonnell, D. G., "Shear-Stress Measurement in Aerodynamic Testing Using Cholesteric Liquid Crystals," Liquid Crystals, Vol. 6, No. 3, 1989, pp. 271-280.

12. Toy, N., Savory, E., and Paskin, S., "The Development of a System for Real-Time, Full-Field Surface Shear Stress Measurements Using Liquid Crystals," Proceedings of the 12th Symposium on Turbulence, University of Missouri-Rolla, MO, 1990.

13. Mee, D. J., Walton, T. W., Harrison, S. B., and Jones, T. V., "A Comparison of Liquid Crystal Techniques for Transition Detection," AIAA Paper 91-0062, Jan. 1991.

14. Reda, D. C., "Observations of Dynamic Stall Phenomena Using Liquid Crystal Coatings," AIAA Journal, Vol. 29, No. 2, Feb. 1991, pp. 308-310.

15. Hall, R. M., Obara, C. J., Carraway, D. L., Johnson, C. B., Wright, E. J., Covell, P. F., and Azzazy, M., "Comparisons of Boundary-Layer Transition Measurement Techniques at Supersonic Mach Numbers, "AIAA Journal, Vol. 29, No. 6, June 1991, pp. 865-871.

16. Parmar, D. S., "A Novel Technique for Response Function Determination of Shear Sensitive Cholesteric Liquid Crystals for Boundary Layer Investigations, "Review of Scientific Instruments, Vol. 62, No. 6, June 1991, pp. 1596-1608.

17. Toy, N., Savory, E., and Disimile, P. J., "Determination of Surface Temperature and Surface Shear Stress Using Liquid Crystals," Proceedings, Forum on Turbulent Flows, ASME JSME Joint Fluids Engineering Conference, Portland, OR, June 1991, pp. 39-44.

18. Reda, D. C., and Aeschliman, D. P., "Liquid Crystal Coatings for Surface Shear-Stress Visualization in Hypersonic Flows," AIAA Journal of Spacecraft and Rockets, Vol. 29, No. 2, March-April 1992, pp. 155-158.

19. Smith, S. C., "Use of Shear-Sensitive Liquid Crystals for Surface Flow Visualization," AIAA J. Aircraft, Vol. 29, No. 2, March-April 1992, pp. 289-293.

20. Wolf, S., Laub, J., King, L., and Reda, D., "Development of NASA-Ames Low-Disturbance Supersonic Wind Tunnel for Transition Research up to Mach 2.5," AIAA Paper 92-3909, 17th Aerospace Ground Testing Conference, Nashville, TN, July 1992.

21. Ward, M. D., Vohra, R., O'Callaghan, M., Roberts, B., and Escher, C., "An Easily Aligned Deformable Helix Ferroelectric Liquid Crystal Mixture and its Use in Devices," SPIE Vol. 1665, Liquid Crystal Materials, Devices, and Applications, 1992, pp. 176-183.

22. Murai, H., Gotoh, T., Suzuki, M., Hasegawa, E., and Mizoguchi, K., "Electro-Optic Properties for Liquid Crystal Phase Gratings," SPIE Vol. 1665, Liquid Crystal Materials, Devices, and Applications, 1992, pp. 230-239.

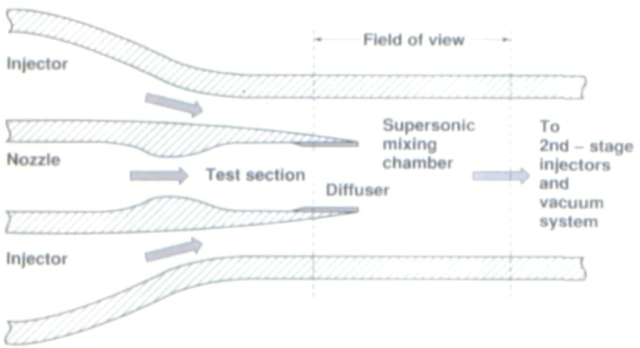

Fig. 1. Schematic of Injector–Driven Wind Tunnel

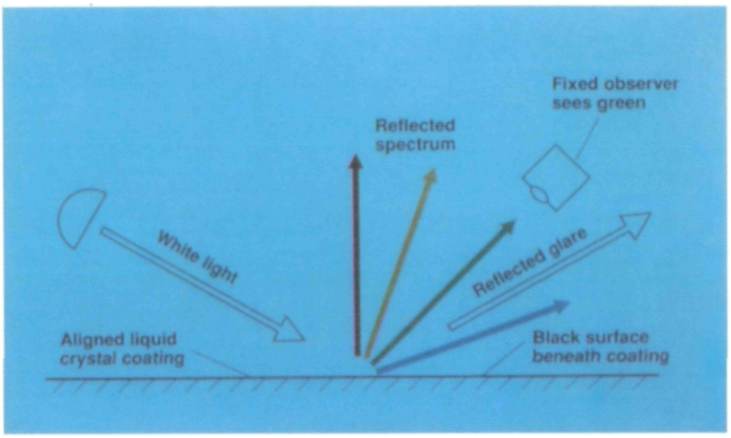

Fig. 2. Liquid Crystal Reflected Spectrum;
Camera Placement in the Absence of Shear

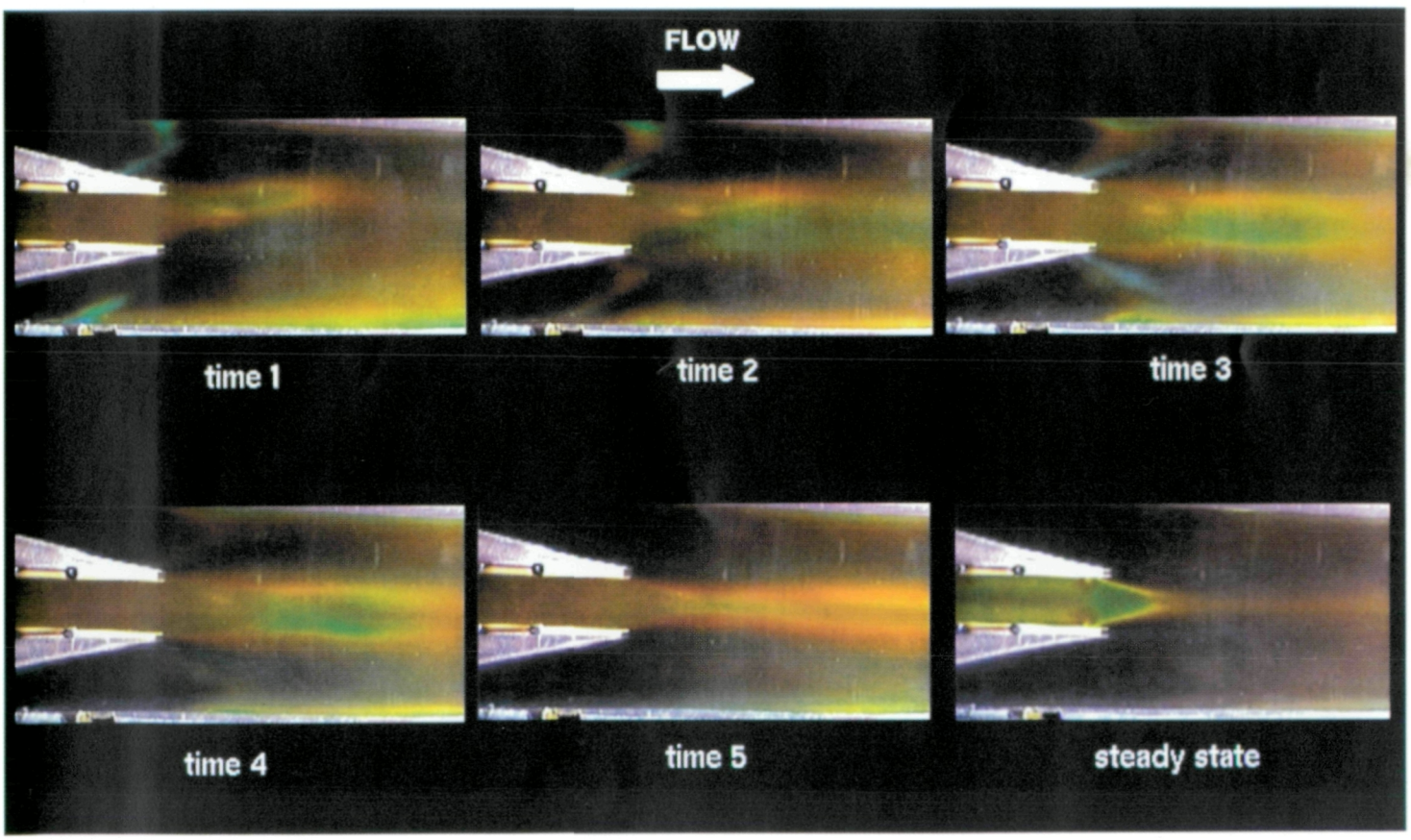

Fig. 3. Liquid Crystal Color Patterns During Tunnel Startup

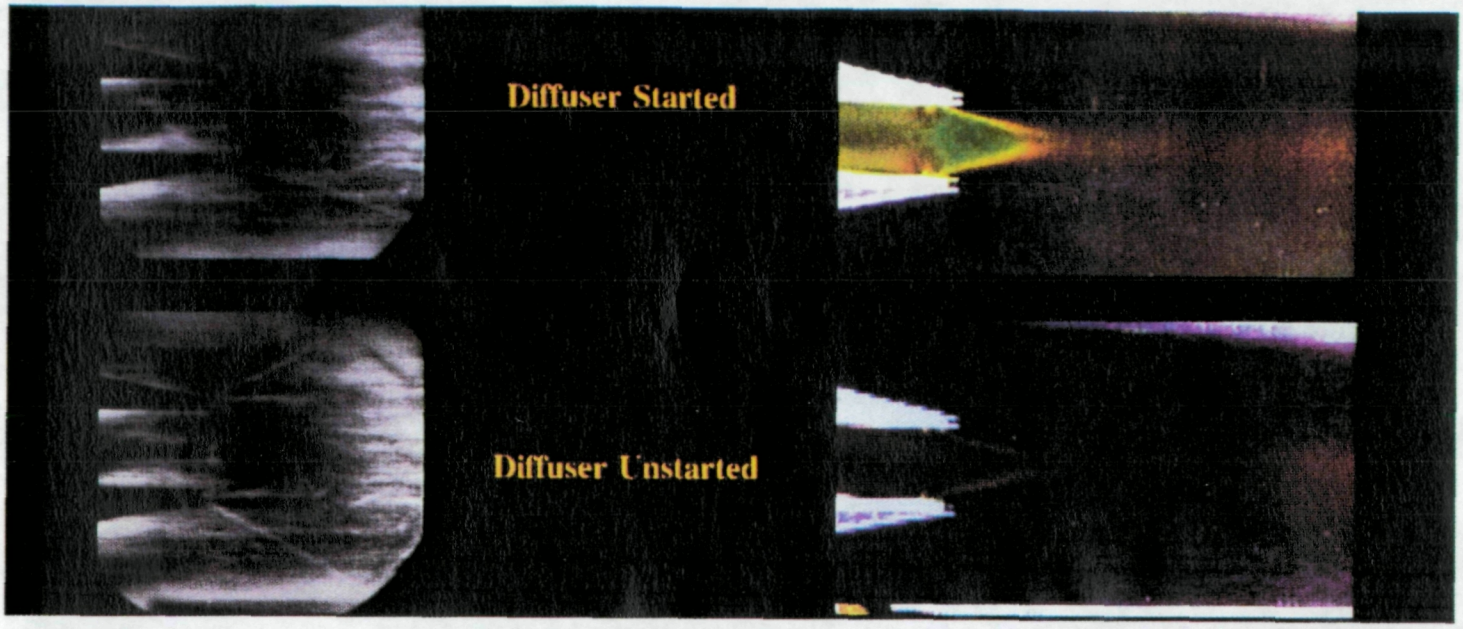

Fig. 4. Schlieren and Liquid Crystal Images Before and During Supersonic Diffuser Unstart

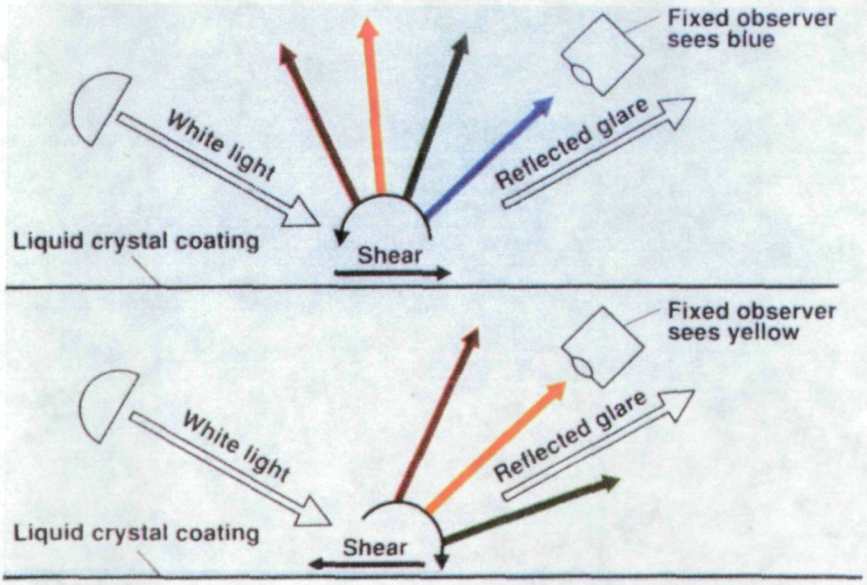

Fig. 5. Reflected Spectrum Rotation as a Function of Shear Direction (Light/Camera/Shear All in Same Plane)

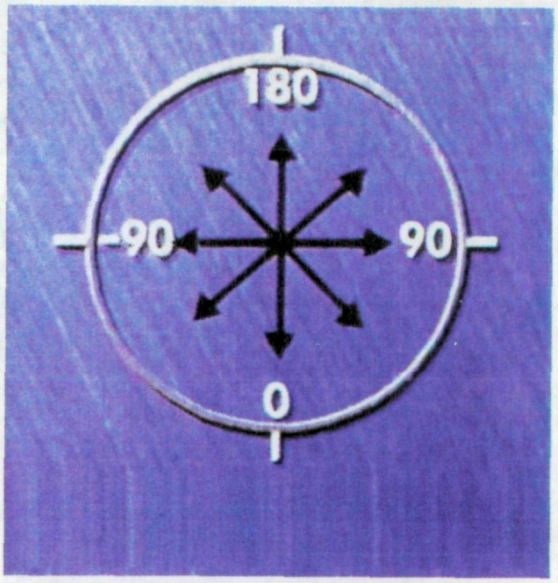

Fig. 6. Case One: Circular Jet Impinging Normal to Flat Surface

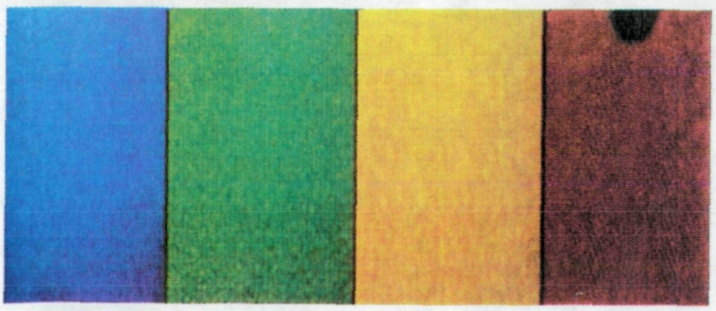

Fig. 7. No-Shear Reflected Colors, Phi = 0 deg., Alpha Increasing Left to Right

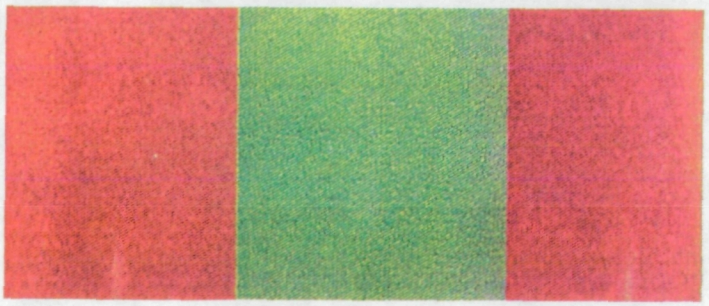

Fig. 8. No-Shear Reflected Colors, Alpha = 45 deg., Phi = -90, 0, +90 deg.

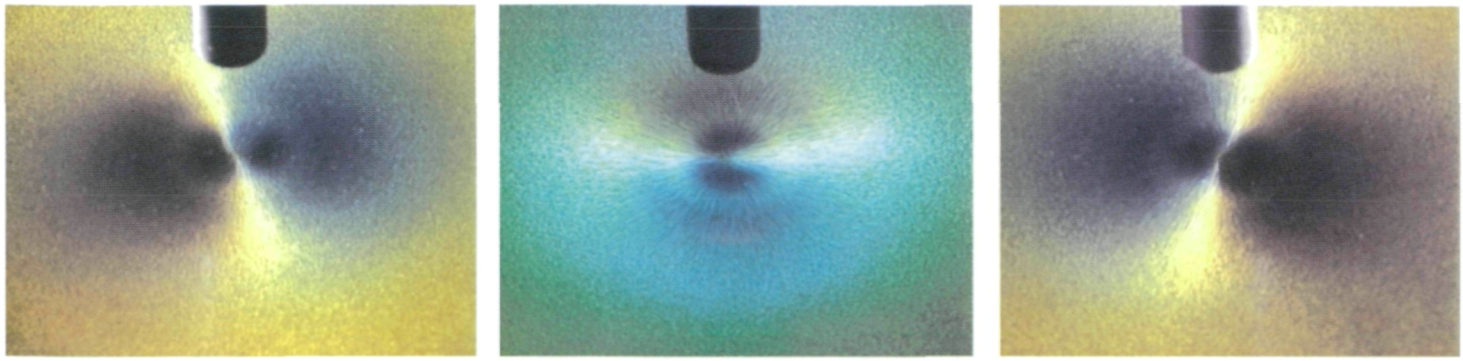

Fig. 9. Shear–Induced Color Patterns Beneath Normal Jet, Phi = –45, 0, +45 deg.

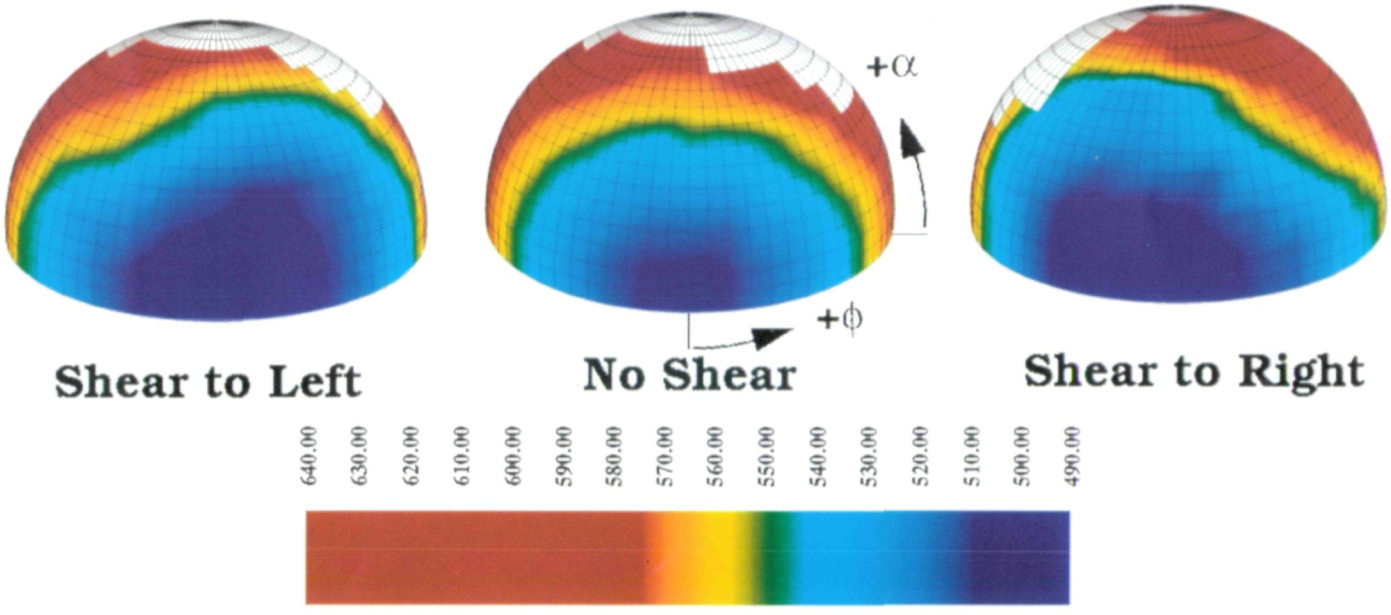

Fig. 10. Spectrophotometer Measurements of Peak–Power Reflected Wavelengths vs. Phi, Alpha View–Angle Combinations

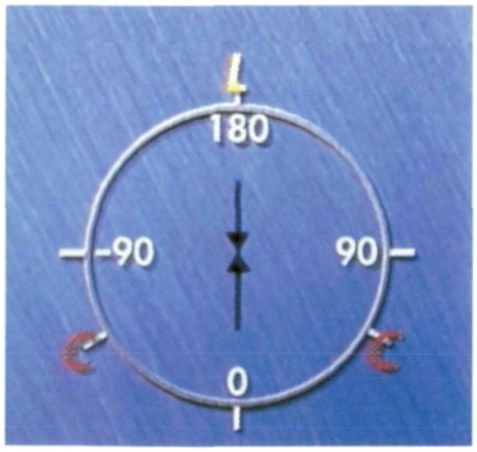

Fig. 11. Light and Tangential Jets Aligned

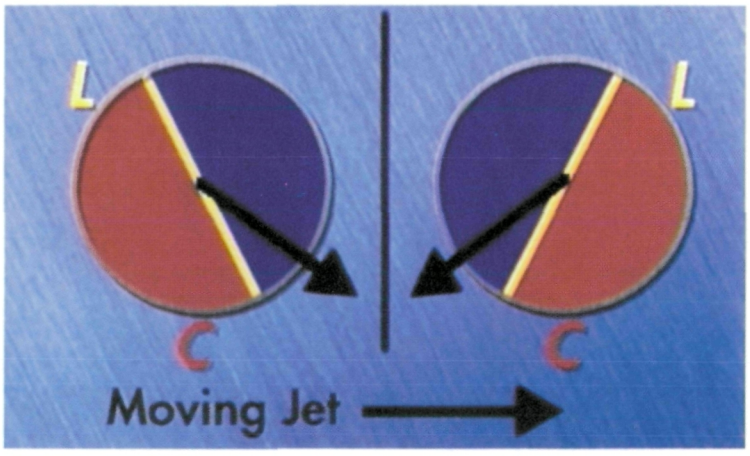

Fig. 12. Normal–Jet–Impingement Color Patterns for Fig. 11

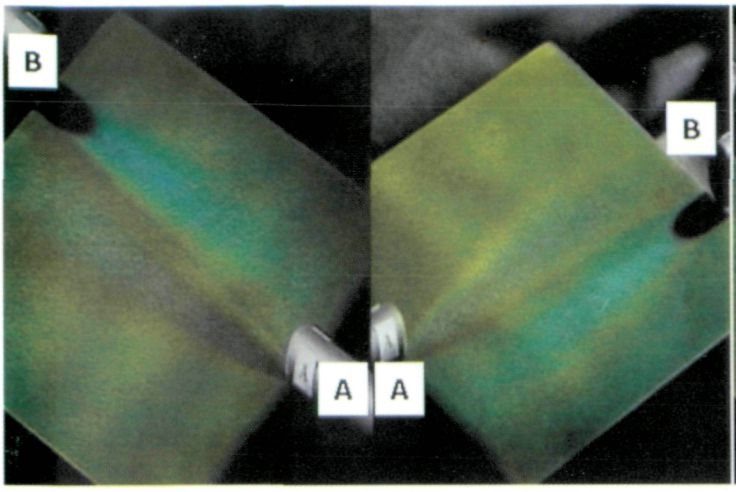

Fig. 13. Tangential–Jet–Induced Color Patterns for Fig. 11, Jets Side by Side

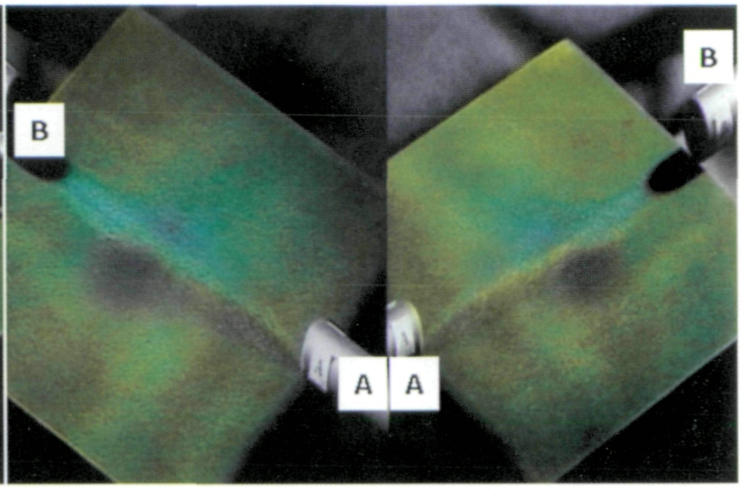

Fig. 14. Tangential–Jet–Induced Color Patterns for Fig. 11, Jets Colliding

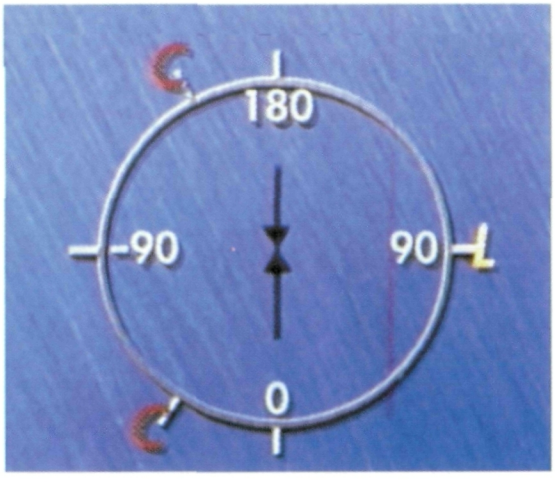

Fig.15. Light and Tangential Jets Perpendicular

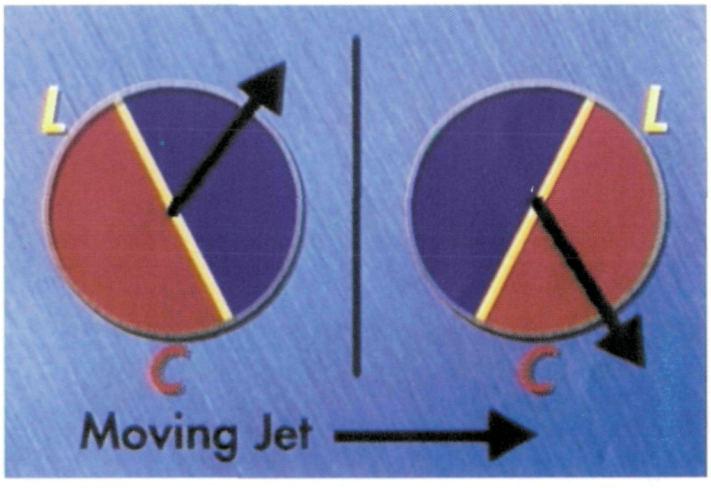

Fig. 16. Normal–Jet–Impingement Color Patterns for Fig. 15

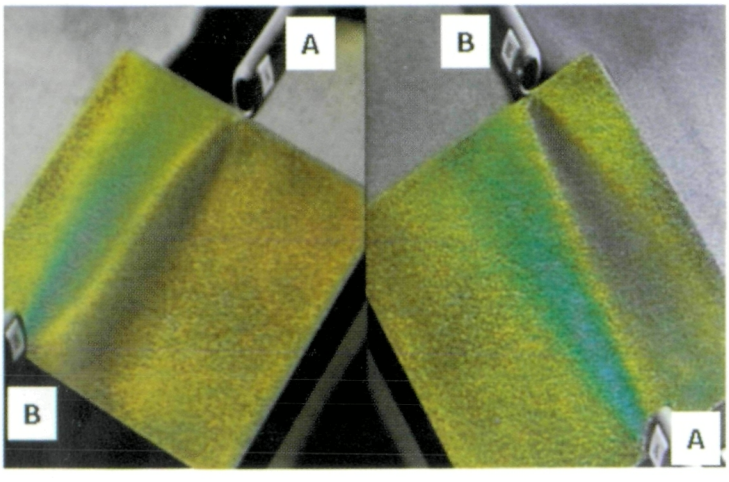

Fig. 17. Tangential–Jet–Induced Color Patterns for Fig. 15, Jets Side by Side

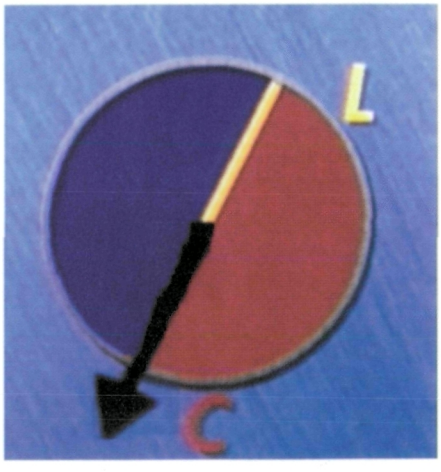

Fig. 18. Extension of Technique to Visualize Small Directional Changes

APPENDIX B

Future Expansion of a Quantified Steady State Flow Field Using Shear-Sensitive Liquid Crystal Coatings

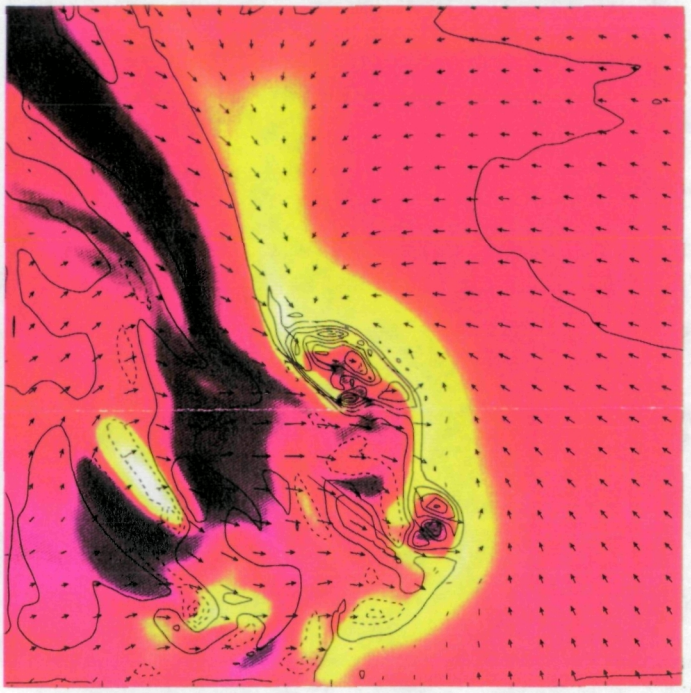

Increasing Shear Magnitude

The above figure is a representation of a steady state 3d boundary layer effects on a test surface coated with a shear-sensitive liquid crystal coating. As is illustrated, the shear magnitude is depicted by a color spectrum and the vector direction at a particular point is indicated by an arrow.